Cysteine Residues in the Human Cannabinoid Receptor: Only C257 and C264 Are Required for a Functional Receptor, and Steric Bulk at C386 Impairs Antagonist SR141716A Binding†

Jonathan F. Fay, Thomas D. Dunham, and David L. Farrens*

Department of Biochemistry and Molecular Biology, Oregon Health and Science University, Portland, Oregon 97239

Received December 31, 2004; Revised Manuscript Received March 28, 2005

ABSTRACT: The human neuronal cannabinoid receptor (CB1) is a G-protein-coupled receptor (GPCR) triggered by the psychoactive ingredients in marijuana, as well as endogenous cannabinoids produced in the brain. As with most GPCRs, the mechanism of CB1 activation is poorly understood. In this work, we have assessed the role of cysteine residues in CB1 ligand binding and activation, and demonstrate a method for mapping key determinants in CB1 structure and function. Through mutational analysis, we find that only two cysteines, C257 and C264, are required for high-level expression and receptor function. In addition, through cysteine reactivity studies, we find that a cysteine in transmembrane helix seven, C386 (C7.42), is reactive toward methanethiosulfonate (MTS) sulfhydryl labeling agents, and is thus solvent accessible. Interestingly, steric bulk introduced at this site, either through MTS labeling or by mutation, inhibits binding of the antagonist drug SR141716A (also known as Rimonabant or Accomplia), but does not affect the binding of the agonist CP55940. Our subsequent modeling studies suggest this effect is caused by steric clash of the modified C386 residue with the piperidine ring of SR141716A and/or disruption of an aromatic microdomain in the binding pocket. On the basis of these results, we hypothesize that bound SR141716A inhibits the ability of transmembrane helix 6 to move during formation of the functionally active receptor state.

The neuronal cannabinoid receptor (CB1) is a G-protein-coupled receptor (GPCR)[1] found at high concentrations throughout the central nervous system (*1*). CB1 is probably best known as the "marijuana receptor", the membrane protein that responds to the psychoactive compounds in *Cannabis sativa*. Activation of cannabinoid receptors has been shown to be involved in numerous physiological processes, including appetite stimulation (*2*). CB1 has also recently been found to play an important role in retrograde neurotransmission, acting to mediate neurotransmitter release in presynaptic terminals by responding to endogenously produced cannabinoid ligands (*3*−*5*). These ligands (derivatives of arachadonic acid) are "made on demand" through the actions of a phospholipase that cleaves them from the phospholipids to which they are attached (*6*−*8*).

Structurally, CB1 exhibits several intriguing anomalies, which together place it in a unique subset of type I GPCRs. These differences include a relatively long N-terminus (∼110 amino acids), which may be involved in receptor stability and/or function (*9*, *10*), the absence of conserved proline residues in transmembrane helices I and V (hereafter termed TMH I and TMH V, respectively), and the presence of a glycine residue in the CWXP motif of TMH VI (*11*). Most strikingly, CB1 also lacks cysteine residues required to make up a highly conserved disulfide bridge thought to connect TMH III with extracellular loop 2 in most GPCRs. In rhodopsin, this disulfide has been confirmed through chemical and crystallographic studies (*12*, *13*) and has been shown to play a key role in the formation of a properly folded, stable receptor (*14*, *15*). Recent studies suggest the inability to form this disulfide bridge may be a key factor in some disease-inducing rhodopsin mutations (*16*).

Although cannabinoid receptors lack the canonical disulfide bond described above, they do appear to contain other conserved cysteine residues. We find through sequence analysis that five cysteine residues are conserved in essentially all cannabinoid receptors.[2] These five residues are

† This research was supported in part by National Institutes of Health Grants EY12095, DA14896, and DA18169.

* To whom correspondence should be addressed: Oregon Health and Science University, Mail Code L224, 3181 S. W. Sam Jackson Park Rd., Portland, OR 97239-3098. Telephone: (503) 494-0583. Fax: (503) 494-8393. E-mail: farrensd@ohsu.edu.

[1] Abbreviations: 1D4 antibody, monoclonal antibody raised against the 18 C-terminal amino acids of rhodopsin; BSA, bovine serum albumin; CP 55,940, (−)-*cis*-3-[2-hydroxy-4-(1,1-dimethylheptyl)-phenyl]-*trans*-4-(3-hydroxypropyl)cyclohexanol; EDTA, ethylenediaminetetraacetic acid; G-protein, guanine nucleotide-binding regulatory protein; GPCR, G-protein-coupled receptor; GTPγS, guanosine 5′-[γ-thio]triphosphate; MMTS, methyl methanethiosulfonate; MTSEA, 2-aminoethyl methanethiosulfonate hydrobromide; PIC, protease inhibitor cocktail; SDS−UPAGE, sodium dodecyl sulfate−urea−polyacrylamide gel electrophoresis; SEM, standard error of the mean; shCB1, synthetic CB1 receptor with an epitope tag; SR141716A, *N*-(piperidin-1-yl)-5-(4-chlorophenyl)-1-(2,4-dichlorophenyl)-4-methyl-1*H*-pyrazole-3-carboxamide HCl; TMH, transmembrane helix; Tris, 2-amino-2-(hydroxymethyl)-1,3-propanediol.

[2] These five cysteine residues are conserved throughout 14 of 16 fully sequenced cannabinoid receptors. The two outliers, zebra fish and Ciona intestinalis CB1, both lack C386 (C7.42). Data analysis was carried out using ClustalW on sequences found in the Swiss-prot and TrEMBL databases.

10.1021/bi0472651 CCC: $30.25
Published on Web 05/25/2005

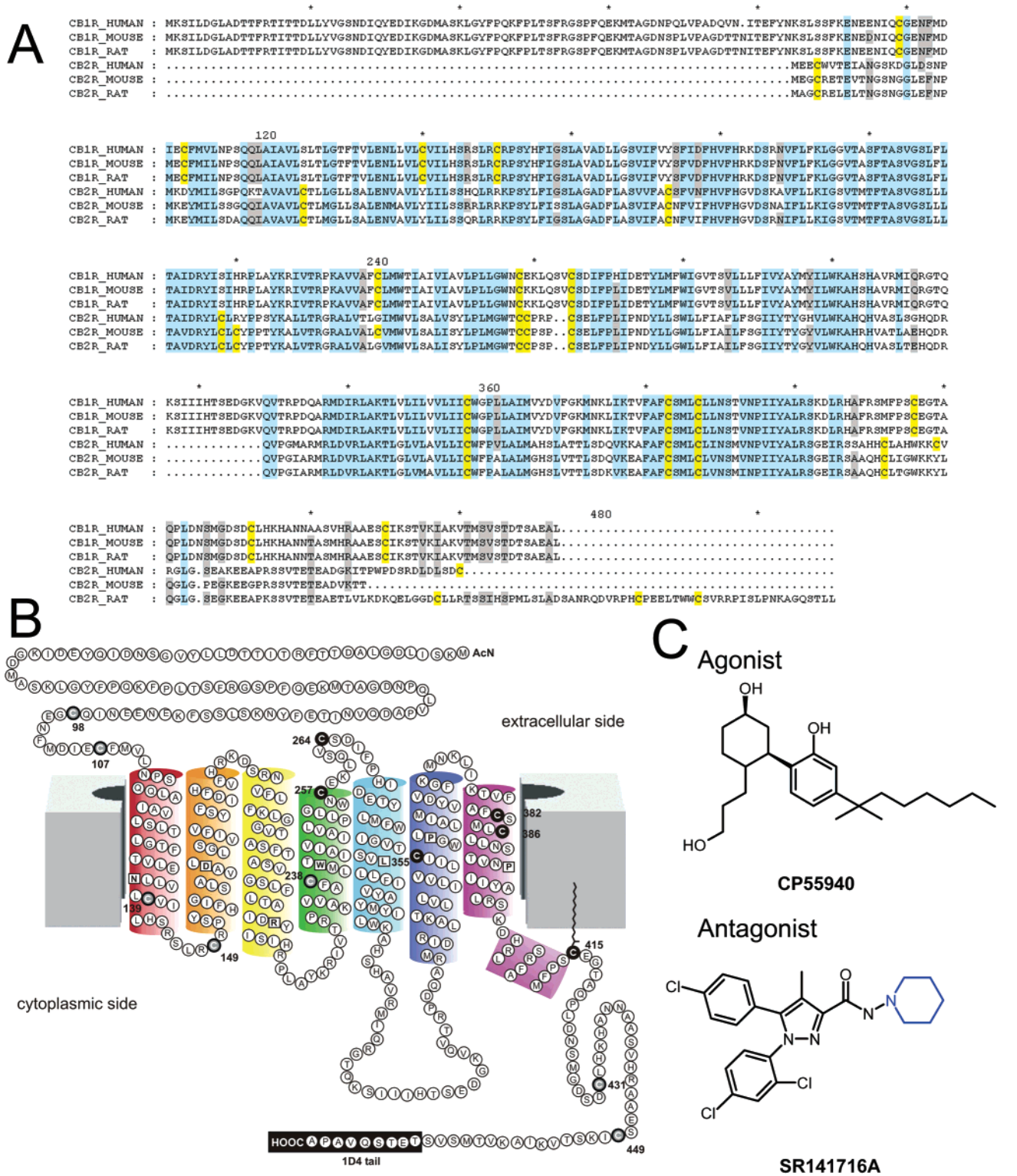

FIGURE 1: (A) Five cysteine residues are conserved in cannabinoid receptors. Comparison alignment of six different cannabinoid receptors. Analysis and alignment were carried out using GeneDoc and ClustalW, based on sequences obtained from the Swiss-protein database. The cysteine residues in cannabinoid receptors are highlighted in yellow. Residues highlighted in light blue are highly conserved similar residues, and residues highlighted in light gray are moderately conserved and less conserved similar residues. (B) Two-dimensional model of the synthetic human CB1 cannabinoid receptor (shCB1-C13). The general organization of the transmembrane helices is adapted from that of Reggio and co-workers (*11*). The cysteine residues are labeled with the residue number. The five cysteine residues conserved in cannabinoid receptors are depicted as black circles. Residues highly conserved in GPCRs, N134 (1.50), D163 (2.50), R214 (3.50), W241 (4.50), L286 (5.50), P358 (6.50), and P394 (7.50), are depicted with boxes and bold letters. (C) Structures of CP55940 (top) and SR141716A (bottom). Note the piperidine ring of SR141716A is highlighted in blue.

shown in Figure 1A, which compares CB1 and CB2 sequences from humans, mice, and rats.

Unfortunately, little is known about the role of cysteine residues in cannabinoid receptors. Early studies found sulfhydryl alkylating agents reduce B_{max} values for cannabinoid agonist binding in rat brain (*17*), and chimera studies have shown two of the conserved CB1 cysteine residues, C257 and C264, are important for ligand binding and for

Table 1: Nomenclature Used for shCB1 Cysteine Mutants

mutant	Cys residues retained in mutant	Ballesteros/Weinstein nomenclature
shCB1-C13 (wild type)	all 13 cysteines	
shCB1-C5	C257, C264, C355, C382, and C386	4.66, 4.73, 6.47, 7.38, and 7.42
shCB1-C2	C257 and C264	4.66 and 4.73
shCB1-C0	all 13 cysteines changed to alanine	
single Cys → Ala mutants in shCB1-C5		
shCB1-C4-355A	C257, C264, C382, and C386	4.66, 4.73, 7.38, and 7.42
shCB1-C4-382A	C257, C264, C355, and C386	4.66, 4.73, 6.47, and 7.42
shCB1-C4-386A	C257, C264, C355, and C382	4.66, 4.73, 6.47, and 7.38
double Cys → Ala mutant in shCB1-C5		
shCB1-C3-386C	C257, C264, and C386	4.66, 4.73, and 7.42

enabling the receptor to be present on the cell surface (*18*). Together, these results have led to the suggestion that C257 and C264 participate in a disulfide bond.

In our work, we set out to systematically characterize the role of endogenous cysteine residues in the CB1 receptor, using a combination of mutational analysis and site-directed labeling studies. We first generated several cysteine to alanine mutants in CB1 to test the potential role of the five conserved cysteine residues (mentioned above) on receptor function. Our results show that only two cysteine residues, C257 and C264, are required for high-level expression and receptor function. We then investigated the sensitivity of the conserved CB1 cysteines to methanethiosulfonate (MTS) sulfhydryl labeling agents and found that one residue, C386 (C7.42), is sensitive to these agents. Our results show that labeling this residue with MTS agents blocks binding of the antagonist drug SR141716A (also known as Rimonabant or Accomplia), as does introducing steric bulk at this site through mutagenesis. Together, our results help further refine models of SR141716A docking in the CB1 receptor (*11*, *19*), enhance development of new derivatives of SR141716A, and set the stage for future site-directed cysteine accessibility studies (for mapping the structure and ligand binding sites of CB1).

EXPERIMENTAL PROCEDURES

Materials. Oligonucleotides were acquired from either Gibco (Carlsbad, CA) or Operon Technologies (Alameda, CA). Deoxynucleotides, restriction enzymes, T4 ligase, and DNA polymerase Vent were purchased from Gibco or NEB (Boston, MA). All buffers were obtained from either Sigma (St. Louis, MO) or Fisher (Springfield, NJ). Materials for gel electrophoresis were bought from either Fisher or Hoefer (San Francisco, CA) with the exception of the 30% acrylamide/bis solution (37.5:1), which was bought from Bio-Rad (Hercules, CA).

Tritiated and untritiated cannabinoid ligands were obtained as a generous gift from the National Institute of Drug Abuse (Research Triangle Park, NC). The protease inhibitor cocktail (PIC) was bought from Roche Diagnostics (Basel, Switzerland). The 1D4 antibody was obtained from the National Cell Culture Center (Minneapolis, MN). MTS compounds were purchased from Toronto Research Chemicals (North York, ON). Goat anti-mouse and anti-rabbit peroxidase-conjugated IgG (H+L) and Super Signal West Pico Luminol/Enhancer Solution were bought from Pierce (Rockford, IL). The N-terminal cannabinoid receptor antibody was bought from Cayman Chemical Co. (Ann Arbor, MI), and the anti-G-protein antibody was bought from Santa Cruz Biotechnology (Santa Cruz, CA).

Buffers. The definitions of the buffers that were used follow: PBSSC (0.137 M NaCl, 2.7 mM KCl, 1.5 mM KH_2PO_4, and 8 mM Na_2HPO_4), "hypotonic buffer" [5 mM Tris-HCl, 2 mM EDTA, and PIC (pH 7.5)], TME [20 mM Tris-HCl (pH 7.4), 5 mM $MgCl_2$, and 1 mM EDTA], "binding buffer" (TME with 5 mg/mL BSA), and "wash buffer" (TME with 1 mg/mL BSA).

Numbering System for Identification of Amino Acid Residues in the CB1 Receptor. The numbering system for identifying amino acid residues in this paper primarily identifies the residue by its number in the CB1 sequence. However, to facilitate reading, the numbering system used by Ballesteros and Weinstein (*20*) has also been employed. In this numbering system, the first number indicates the transmembrane helix and the second number, following a period, indicates the most conserved residue in each helix as 50. From the conserved residue, numbers either descend or ascend to the N-terminus or to the C-terminus, respectively. Thus, in this nomenclature, the conserved residues denoted as 50 are N134(1.50), D163(2.50), R214(3.50), W241(4.50), L286(5.50), P358(6.50), and P394(7.50). The locations of these residues are highlighted in Figure 1B.

Nomenclature and Rationale for Construction of shCB1 Cysteine Mutants. The putative locations of the 13 cysteine residues in CB1 are shown in Figure 1B. In this paper, the "wild-type" shCB1 construct, which contains all of the 13 native cysteine residues, is called shCB1-C13. To investigate the role of these cysteine residues and to facilitate further site-directed labeling experiments, we constructed a CB1 mutant in which eight of these 13 residues were mutated to alanines, called shCB1-C5. In shCB1-C5, cysteine residues 257 and 264 were retained because of their potential role in forming a disulfide (*18*). Residues 355, 382, and 386 were retained because these residues are conserved between CB1 and CB2 (see Figure 1A), and also because model structures suggest that these three residues point inward toward each other in the helical bundle, indicating they might play some functional role in ligand binding. The shCB1-C2 construct was made to contain only the two cysteines involved in the putative disulfide. Finally, a complete Cys-less CB1 mutant, shCB1-C0, was constructed to test if any cysteine residues were required for functional CB1. Further MTS reactivity studies led to the construction of several other shCB1 mutants for identification of reactive cysteine residues. These mutants (described above) are denoted in Table 1.

Construction of Cysteine Receptor Mutants. The construction of the wild-type CB1 receptor gene, called shCB1 (or in this paper shCB1-C13), has previously been described (*21*). In the work presented here, all of the cysteine to alanine

substitutions were carried out by changing the cysteine codon (TGC) to the alanine codon (GCC) in this gene (*21*). Briefly, this involved first constructing mutant shCB1-C7 (C98, C107, C257, C264, C355, C382, and C386) by following a multistep PCR method (*21*), in which 12 40mer oligonucleotides containing the Cys → Ala mutations were added to the remaining 62 oligonucleotides required to construct the shCB1 gene. The oligonucleotide mixture was subjected to two rounds of PCR. The first round linked the oligos together to create a template, and the second amplified the diluted template with a pair of flanking primers. The resulting PCR fragment was extracted from a 1% agarose gel using a gel purification kit (Qiagen). Introduction of subsequent Cys → Ala mutations was carried out using a QuikChange PCR protocol (Stratagene, La Jolla, CA) and the shCB1-C7 construct as the template. The resulting purified gene products were cloned into the PMT4 vector using the *Eco*RI and *Not*I restriction sites that flank the gene.

The shCB1-C5 mutant was created gradually by incorporating the N-terminal coding region of the QuikChange product (C98A and C107A) into the shCB1-C7 construct using *Eco*RI and *Sca*I restriction sites. The creation of shCB1-C2 was accomplished by inserting a fragment containing C355A, C382A, and C386A mutations into shCB1-C5 using *Spe*I and *Not*I sites. shCB1-C0 was created by replacing C257 and C264 with alanines in the shCB1-C2 construct utilizing their shared *Kpn*I and *Cla*I restriction sites. The shCB1-C4-386A and shCB1-C3-386C constructs were made by incorporating the appropriate fragments into shCB1-C5 using their *Bam*HI and *Apa*I sites. The shCB1-C4-355A and shCB1-C4-382A mutants were constructed using shCB1-C5 as a template in a QuikChange PCR protocol. The shCB1-C12-386M mutant was also constructed using the QuikChange protocol with shCB1-C13 as the template. All restriction digests were resolved with a 1% agarose gel and purified using a gel purification kit (Qiagen). Digested fragments were ligated with T4 DNA ligase (Invitrogen) and transformed into DH5α competent cells. The sequence of the purified DNA plasmids was confirmed before use.

Construction of shCB1−Gα$_i$ Cysteine Mutants. To facilitate functional assays, the shCB1 cysteine mutants were studied using a G-protein chimera system developed for GTPγS binding assays (*21*). This system employs a fusion gene construct in which the N-terminus Gα$_i$ sequence is tethered to the C-terminus of the CB1 gene. Mutant shCB1 constructs were PCR amplified as described previously (*21*). In brief, each cysteine mutant was amplified using two sets of fusion primers. To facilitate this work, the *Xho*I restriction site was introduced as a linker and adaptor between shCB1 and Gα$_i$. The purified mutant PCR products that were obtained were digested with restriction enzymes and subcloned into the shCB1−Gα$_i$ plasmid vector construct using the *Eco*RI and *Xho*I restriction enzymes for both the PCR products and vector. Products were then ligated and sequenced as described above.

Transfection, Expression, and Preparation of shCB1 Cell Membranes. All the shCB1 mutants were expressed in COS-1 cells using a DEAE-dextran-based transient transfection method as previously described (*21*−*23*). Fifty-six hours after transfection, the shCB1-transfected cell monolayers were washed twice with 10 mL of PBSSC, then harvested, and centrifuged; either the monolayers were used immediately, or the cell pellets were snap-frozen in liquid nitrogen and stored at −80 °C until they were used.

Membranes expressing the shCB1 cysteine mutants were prepared for binding studies as previously described (*21*). Briefly, cell pellets were homogenized using 30 strokes in a glass mortar and pestle in a final volume of 1 mL of hypotonic buffer per plate, and then subjected to centrifugation for 45 min at 40000*g*. After centrifugation, the pellets were washed with 5 mL of TME and resuspended via homogenization in TME with PIC, and the protein concentration was determined using the modified DC protein assay kit (Bio-Rad). Membrane preparations were frozen in liquid nitrogen as aliquots and stored at −80 °C until they were used.

Quantitative Immunoblot Analysis (QIB). To compare expression levels of different mutants, the total amount of expressed shCB1 polypeptide was determined using quantitative Western blot analysis, as previously described (*21*). Known concentrations of rhodopsin standards were run on a SDS−UPAGE gel along with unknown concentration of shCB1 mutants, and then the gel was transferred to Immobilon-P membranes and immunoblotted with the 1D4 antibody, which recognizes the TETSQVAPA C-terminal amino acid sequence. The blots were then incubated with peroxidase-conjugated goat anti-mouse IgG (H+L) (Pierce), and visualized using enhanced chemiluminescence. The relative intensities of the standards and unknowns were determined via pixel density using a Bio-Rad Phosphoimager Screen CH, GS-525 molecular imaging system, and supplied software (Bio-Rad). Quantitations of the expressed protein were calculated assuming a molecular mass for rhodopsin of 42 000 Da and for shCB1 of 52 800 Da. Data were fit with linear regression algorithms supplied in Sigma Plot software (SPSS Science, Chicago, IL). Alternatively, Western blots for the N-terminus and Gα$_i$ C-terminus were visualized with KODAK X-OMAT AR film.

Radioligand Binding Studies. The ligand binding characteristics of the shCB1 and shCB1−Gα$_i$ membrane preparations were measured using a previously described competitive inhibition binding assay (*21*). In brief, membranes (50 μg of total membrane protein/data point) were incubated at 30 °C for 1 h (final assay volume of 500 μL) in a reaction mix comprised of binding buffer and ∼0.5 nM tritiated reporter ligand in the presence of increasing amounts of agonist or antagonist. Binding was terminated by adding 4.5 mL of wash buffer, then rapidly filtering over Whatman GF/B filters [pretreated with polyethyleneimine 0.2% (w/v)] using a Brandel 24-well filtration apparatus, and then washing the filters two more times with 5 mL of wash buffer. All rapid filtration was performed at 4 °C with buffers maintained on ice; pipet tips and all glass test tubes were silanized. Radioactivity was detected and quantified by the liquid scintillation counting method. Data were fit using the Swillens approximation, which takes into account ligand depletion and employs a nonlinear regression algorithm for the following equation:

$$b^*_{tot} = \frac{r_{tot}L^*}{K_d + L^* + L} + L^*_{cpm}\alpha$$

where b^*_{tot} is the concentration of bound radioligand (counts per minute), r_{tot} is the B_{max} (counts per minute), L^* is the

concentration of free ligand (nanomolar), L is the concentration of free unlabeled ligand (nanomolar), L^*_{cpm} is the concentration of free ligand (counts per minute), and α is the ratio of nonspecific bound to free ligand (*24*). Data were also fit to the one-site competition equation utilized by the pharmacology features in Sigma Plot where the K_d and B_{max} values were estimated using the following equations:

$$K_d = IC_{50} - L^*_o \text{ and } B_{max} = \frac{B_0 IC_{50}}{L^*_o}$$

where L^*_o is the concentration of radioligand and B_0 is the concentration of specific bound radioligand (*25*).

Agonist Stimulation of [35S]GTPγS Binding by the shCB1−Gα$_i$ Fusion Protein. The ability of cannabinoid agonist CP55940 to stimulate GTPγS incorporation in the shCB1−Gα$_i$ fusion protein was assessed using a filter binding assay previously described with some modifications (*21*). Briefly, membranes (50 μg) were incubated at 30 °C for 45 min (final assay volume of 500 μL) in a reaction mix of binding buffer, with 100 mM NaCl, 100 μM GDP, 300 pM [γ-^{35}S]GTP, and an increasing amount of agonist, CP55940. Binding was terminated by the addition of 4.5 mL of ice-cold wash buffer, followed by rapid filtering through prewetted (rinsed with 5 mL of wash buffer) Whatman GF/B filters. Membranes were washed once more with 5 mL of ice-cold wash buffer. The EC_{50} was determined by using the sigmoidal dose−response equation found in the Sigma Plot pharmacology package.

Treatment of shCB1 Cysteine Mutants with Methanethiosulfonate (MTS) Reagents. Treatment of the shCB1 cysteine mutants with sulfhydryl specific methanethiosulfonate (MTS) derivatives was performed in parallel with untreated samples. Control groups were treated with an equal volume of the TME buffer. Prior to the assays, appropriate amounts of MTS reagents (in powdered form) were weighed out and stored desiccated at −20 °C, and then brought up in TME buffer immediately before use, as described previously (*26*). Before the radioligand binding studies, 900 μg of total membrane was treated with 50 mM MMTS or 20 mM MTSEA in TME and PIC (600 μL). This reaction mixture was allowed to mix at room temperature for 10 min on a nutator, and then a 500 μL aliquot of this sample was immediately diluted into binding buffer to a final volume of 4.5 mL. From this stock, 150 μL was added to 350 μL of the binding mix (25 μg of total membrane protein), and filtration binding studies were carried out as described above. The data represent either the mean of two binding experiments fit to the one-site competition equation found in Sigma Plot or the specific percent bound utilizing the average minimum and maximum values in contrast to untreated membranes minimum and maximum values.

Molecular Modeling. Coordinates for an empty CB1 receptor model were generously provided by O. M. Salo (*27*). In the work presented here, we altered this CB1 model as follows. The aromatic rings of W6.48 and F3.36 were stacked gauche$^+$ and trans, as suggested for the inactive state (*27*, *28*). The antagonist SR141716A was constructed using ISIS ChemDraw and then minimized using a Dreiding force field (for 25 000 iterations at a convergence criterion of 0.0001), followed by applying the "clean" feature using DS Viewer Pro and the Conformer 5.05 module (Accelrys Inc.). This minimized SR141716A was then docked into the aromatic microdomain of the CB1 model and the carboxamide oxygen of SR141716A aligned with K192, as this lysine is important for SR141716A binding (*11*). Initial docking of SR141716A was carried out manually using the following distance parameters that describe centroid to centroid distances from the monochloro (MC) or dichloro (DC) rings in SR141716A to the residues in CB1 under discussion. Monochloro ring MC: F3.36, d = 8.2 Å; Y5.39, d = 6.06 Å; W5.43, d = 5.37 Å; and W6.48, d = 12.65 Å. Dichlorophenyl ring DC: F3.36, d = 4.42 Å; Y5.39, d = 8.46 Å; W5.43, d = 4.07 Å; W6.48, d = 8.52 Å; and carboxamide oxygen of SR141716A with K3.28 (N−O distance), 2.71 Å.

After this initial dock, amino acids within 15 Å of the docked ligand were selected, and the protein backbone was frozen. The model was then subjected to a Dreiding force field (for 5000 iterations at a convergence criterion of 1) followed by application of the "clean" feature (as described above). This produced the final distance parameters. Monochloro ring MC: F3.36, d = 9.41 Å; Y5.39, d = 6.28 Å; W5.43, d = 6.36 Å; and W6.48, d = 13.38 Å. Dichlorophenyl ring DC: F3.36, d = 5.22 Å; Y5.39, d = 7.55 Å; W5.43, d = 3.62 Å; W6.48, d = 9.17 Å; and carboxamide oxygen of SR141716A with K3.28 (N−O distance), 3.19 Å.

RESULTS

Construction of shCB1 Cysteine Mutants. The studies described here all employed a synthetic gene of CB1, called shCB1 (*21*). In this paper, we refer to cysteine mutants in this gene as shCB1-C#, where C# refers to the number of remaining cysteines present in the construct. For example, the wild-type native human CB1 receptor contains 13 cysteine residues; thus, it is called shCB1-C13. In the construction of CB1 mutants, the cysteine residues to be investigated were replaced with alanines (Table 1). The first construct, shCB1-C5, was created to retain the five cysteine residues (Figure 1 A) conserved in cannabinoid receptors (C257, C264, C355, C382, and C386). Mutant shCB1-C2 was created to contain only the two cysteines thought to be involved in a disulfide bond, C257 and C264 (*18*). Finally, a mutant was created in which all 13 residues were replaced with alanines, called shCB1-C0.

Expression and Characterization of shCB1 Cysteine Mutants. The shCB1 mutants were transiently expressed in COS-1 cells and produced between 20 and 90 pmol/mg of total membrane protein (or 5−20 μg/15 cm plate), as verified by quantitative Western blot analysis (Table 2). These receptors were full-length, as indicated by Western blot analysis, which confirmed the presence of both the C- and N-termini (Figure 2, inset). The mutant constructs had no abnormal gel patterns and mobilities of ∼51 kDa, consistent with previously published values (*18*, *21*).

The ligand binding plots for the mutants are shown in Figure 2, presented as the specific picomoles per milligram of total membrane protein, to indicate the quality of the "raw" data (note that the appearance of the plots can be affected by variations in receptor expression levels, ligand affinity, functionality, and the amount of radioligand used in each experiment). The K_d and B_{max} values obtained from these experiments, shown in Table 2, indicate the ligand binding

Table 2: K_d and B_{max} Values for shCB1 and shCB1 Cysteine Mutants Transiently Expressed in COS-1 Cells[a]

receptor construct	CP55940 K_d (nM)	CP55940 B_{max} (pmol/mg of total protein)	SR141716A K_d (nM)	SR141716A B_{max} (pmol/mg of total protein)	QIB[b] (pmol/mg of total protein)
shCB1-C13	5.5 ± 2.7	3.4 ± 1.3	2.8 ± 0.2	5.5 ± 0.1	21.8 ± 3.3
shCB1-C5	12.2 ± 0.2	7.9 ± 1.0	2.1 ± 0.1	12.7 ± 1.5	79.0 ± 20.0
shCB1-C2	2.0 ± 0.4	2.7 ± 0.6	2.0 ± 0.3	7.9 ± 2.2	56.5 ± 26.5
shCB1-C0	4.3 ± 2.1[c]	0.8 ± 0.1[c]	*d*	*d*	89.0 ± 10.0

[a] Data obtained from [^{3}H]CP55940 and [^{3}H]SR141716A competitive displacement binding studies. For comparison purposes, B_{max} values obtained from quantitative immunoblot analysis (QIB) are also presented. Competitive displacement binding assays were performed, and K_d and B_{max} values were calculated as described in Experimental Procedures. Data represent the mean ± SEM of two independent experiments, each performed in duplicate. [b] Quantitative immunoblot analysis (QIB) values indicate the total amount of expressed shCB1 polypeptide, regardless of its ability to bind ligand. [c] Data not fit using the Swillens approximations for ligand depletion. [d] Cys-less mutant shCB1-C0 displayed no detectable [^{3}H]SR141716A binding using the conditions described in Experimental Procedures.

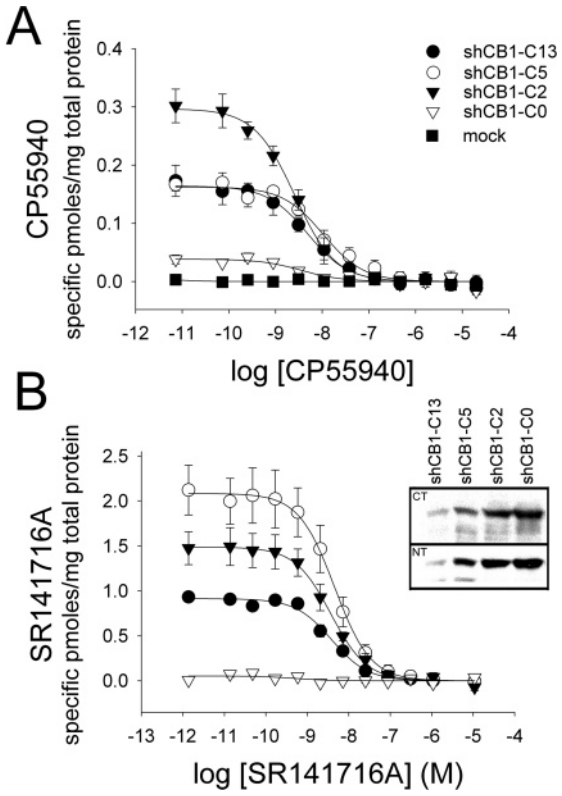

FIGURE 2: Competitive inhibition binding studies of the shCB1 cysteine mutants. The data are for the wild-type or shCB1-C13 receptor (●) and mutants shCB1-C5 (○), shCB1-C2 (▼), and shCB1-C0 (▽) in COS-1 transiently transfected cell lines. The mock data (■) represent ligand binding properties of untransfected COS-1 cells. (A) Homologous displacement binding study of the agonist CP55940. (B) Homologous displacement binding study of the antagonist SR141716A. Data represent the mean of two binding experiments performed in duplicate ± SEM. For details, see Experimental Procedures and Table 2. The inset shows N-terminal and C-terminal Western blots of the shCB1 cysteine mutants. The data indicate shCB1-C5 and shCB1-C2 are similar to wild-type shCB1-C13, whereas shCB1-C0 has impaired binding.

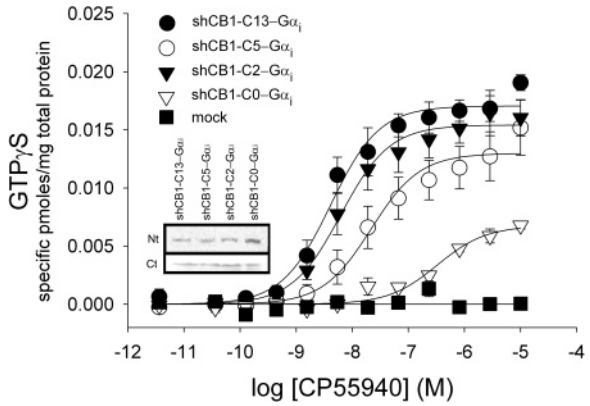

FIGURE 3: Stimulation of GTPγS binding by cysteine mutants introduced into a shCB1−Gα_i fusion protein. The data show agonist-stimulated GTPγS binding of the wild type or shCB1-C13−Gα_i (●) and mutants shCB1-C5−Gα_i (○), shCB1-C2−Gα_i (▼), and shCB1-C0−Gα_i (▽) in COSH-1 transiently transfected cell lines. The mock data (■) represent GTPγS binding properties of untransfected COS-1 cells. The data indicate that all but two cysteines, C257 and C264, can be replaced in CB1 while still retaining a functional receptor. Data represent the mean of two filter binding experiments performed in duplicate ± SEM. For details, see Experimental Procedures and Table 3. The inset shows a N-terminal and C-terminal Western blots showing the shCB1−Gα_i fusion cysteine mutants.

Table 3: EC_{50} for Agonist (CP55940)-Induced [^{35}S]GTPγS Binding by shCB1−Gα_i and shCB1−Gα_i Cysteine Mutants[a]

receptor construct[b]	CP55940 EC_{50} (nM)
shCB1-C13−Gα_i	4.3 ± 0.9
shCB1-C5−Gα_i	23.5 ± 7.4
shCB1-C2−Gα_i	6.8 ± 1.7
shCB1-C0−Gα_i	365.7 ± 140.5

[a] Agonist-induced GTPγS incorporation binding assays were performed, and EC_{50} values were calculated as described in Experimental Procedures. Data represent the mean ± SEM of two independent experiments, each performed in duplicate. [b] See Experimental Procedures for the nomenclature.

characteristics of mutants shCB1-C5 and shCB1-C2 are similar to those of the wild type, shCB1-C13. In contrast, the cysteine-less mutant, shCB1-C0, appeared to have no antagonist binding, and a greatly reduced agonist B_{max} value, despite the fact that Western blot analysis indicated that a full-length polypeptide was produced (Figure 2 and Table 2).

Expression and Characterization of Cysteine Mutants as shCB1−Gα_i Fusion Proteins. The functional ability of the cysteine mutants (i.e., their ability to activate G-protein) was assessed by fusing the mutant shCB1 gene with a Gα_i subunit, to produce a shCB1−Gα_i fusion construct. These fusion proteins were then used to assess the ability of the agonist CP55940 to stimulate GTPγS binding (*21*). The mutant constructs shCB1-C5, shCB1-C2, and shCB1-C0 were cloned into the shCB1−Gα_i fusion construct, expressed in COS-1 cells, and verified by anti-CB1 antibodies for the N-terminal and anti-Gα antibodies for the C-terminal region (Figure 3, inset). All the constructs were expressed as full-length proteins, which exhibited molecular masses of ~90 kDa and bound agonist and antagonist ligands with wild-type-like affinities. The only exception was the shCB1 mutant

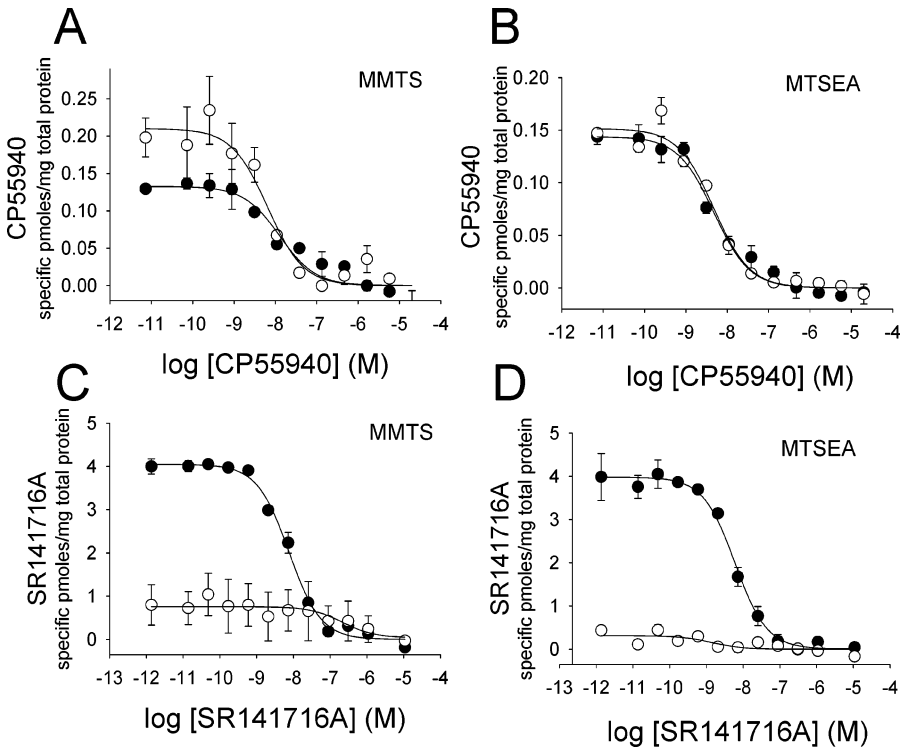

FIGURE 4: Effect of MTS reagents on the ligand binding ability of wild-type shCB1-C13. These results indicate that MTS reagents impair antagonist binding for shCB1-C13. Competitive inhibition binding studies of shCB1-13 for agonist (A and B, top) and antagonist (C and D, bottom) in the presence (○) or absence (●) of a 10 min application of 50 mM MMTS (A and C, left) or 20 mM MTSEA (B and D, right). Data represent the mean of two binding experiments ± SEM, with approximately 25 μg of the total membrane protein used per data point.

lacking all cysteines (shCB1-C0−$G\alpha_i$), which exhibited B_{max} values 3- or 10-fold lower than that for shCB1-C13−$G\alpha_i$ for CP55940 or SR141716A binding, respectively (data not shown).

Ability of Cysteine Mutants in the shCB1−$G\alpha_i$ Fusion Protein To Induce GTPγS Binding. The shCB1−$G\alpha_i$ fusion proteins were assayed for their ability to stimulate GTPγS binding as a function of high-affinity agonist CP55940 concentration. shCB1-C5−$G\alpha_i$ and shCB1-C2−$G\alpha_i$ mutants were found to be functional, as they responded to agonist like the wild-type shCB1-C13−$G\alpha_i$ mutant (see Figure 3 and Table 3). In contrast, the cysteine-less construct, shCB1-C0−$G\alpha_i$, induced only a small amount of GTPγS incorporation (~25% of shCB1-C13−$G\alpha_i$ incorporation), and exhibited a decrease in potency as indicated by the shift to the right of the EC_{50} value (from 5−25 to ~360 nM; see Figure 3 and Table 3).

Effect of Methanethiosulfonate (MTS) Cysteine-Modifying Reagents on shCB1 Mutants. We next assessed whether cysteine residues in CB1 were close to ligand binding sites, by measuring the effect of sulfhydryl specific methanethiosulfonate (MTS) agents. As shown in Figure 4, application of a large positively charged label (MTSEA) or a small neutral label (MMTS) did not dramatically alter agonist (CP55940) binding in the wild-type mutant shCB1-C13 under our conditions. However, we note that interpreting the effect of MTS labeling on agonist binding studies is difficult, because one cannot clearly determine if the cysteine labeling reagents are affecting the cysteine residues in CB1 or the bound G-protein (which is known to enhance agonist binding in CB1). Thus, in our subsequent studies, we only focused on assessing the effect of MTS reagents on antagonist binding in CB1.

In contrast to their minimal effect on agonist binding, we found that MMTS and MTSEA labeling dramatically impaired binding of antagonist SR141716A to wild-type shCB1-C13. Similarly, mutant shCB1-C5, which contains only the five conserved cysteines, was also affected by these MTS agents. To identify which of the remaining five cysteine residues in shCB1-C5 caused sensitivity to the MTS agents, we constructed and tested a series of single-cysteine mutants within the shCB1-C5 construct. These mutants are denoted as shCB1-C4, followed by the mutated residue: shCB1-C4-355A, shCB1-C4-382A, and shCB1-C4-386A. All of these mutants were expressed well in COS-1 cells, bound agonist and antagonist at wild-type-like affinities (Table 4), and appeared to have the molecular mass of a full-length protein (Figure 5C).

As shown in Figure 5, of these shCB1-C4 mutants, only shCB1-C4-386A was completely insensitive to MTS reagents. These results strongly suggest C386 reacts with the MTS labels, and that labeling this residue impairs the ability of shCB1 to bind antagonist SR141716A. To further confirm this hypothesis, we introduced a cysteine at position 386 back into the nonreactive shCB1-C2 construct, resulting in mutant shCB1-C3-386C. As expected, the introduction of C386 back into shCB1-C2 restored the sensitivity to the MTS reagents (Figure 5).

Steric bulk at C386 impairs antagonist binding but not agonist binding. The MTS labeling studies described above suggest antagonist binding to the CB1 receptor is sensitive to steric bulk around residue C386. To further explore this possibility, we next introduced a methionine residue at position 386. This mutation (C386M) was constructed in the shCB1-C13 background, and the construct is hereafter called shCB1-C12-C386M. This mutant was expressed well in

Table 4: K_d and B_{max} Values for shCB1-C4 Cysteine Mutants Transiently Expressed in COS-1 Cells[a]

receptor construct	CP55940 K_d (nM)	CP55940 B_{max} (pmol/mg of total protein)	SR141716A K_d (nM)	SR141716A B_{max} (pmol/mg of total protein)	QIB[b] (pmol/mg of total protein)
shCB1-C4-355A	4.7 ± 0.4	4.4 ± 1.3	3.3 ± 0.04	8.4 ± 0.62	76
shCB1-C4-382A	4.1 ± 0.1	6.2 ± 0.8	4.8 ± 0.26	20.6 ± 1.4	99
shCB1-C4-386A	3.6 ± 0.2	6.0 ± 1.1	5.4 ± 0.51	22.2 ± 0.4	65
shCB1-C3-386C	5.0 ± 0.9	4.4 ± 1.0	3.1 ± 0.4	16.6 ± 7.5	51.5

[a] For comparison purposes, quantitative immunoblot analysis (QIB) values are also reported. Competitive displacement binding assays were performed, and K_d and B_{max} values were calculated using the one-site competition equation described in Experimental Procedures. Data represent the mean ± SEM of two independent experiments, each performed in duplicate. [b] Quantitative immunoblot analysis (QIB) values indicate the total amount of expressed shCB1 polypeptide, regardless of its ability to bind ligand.

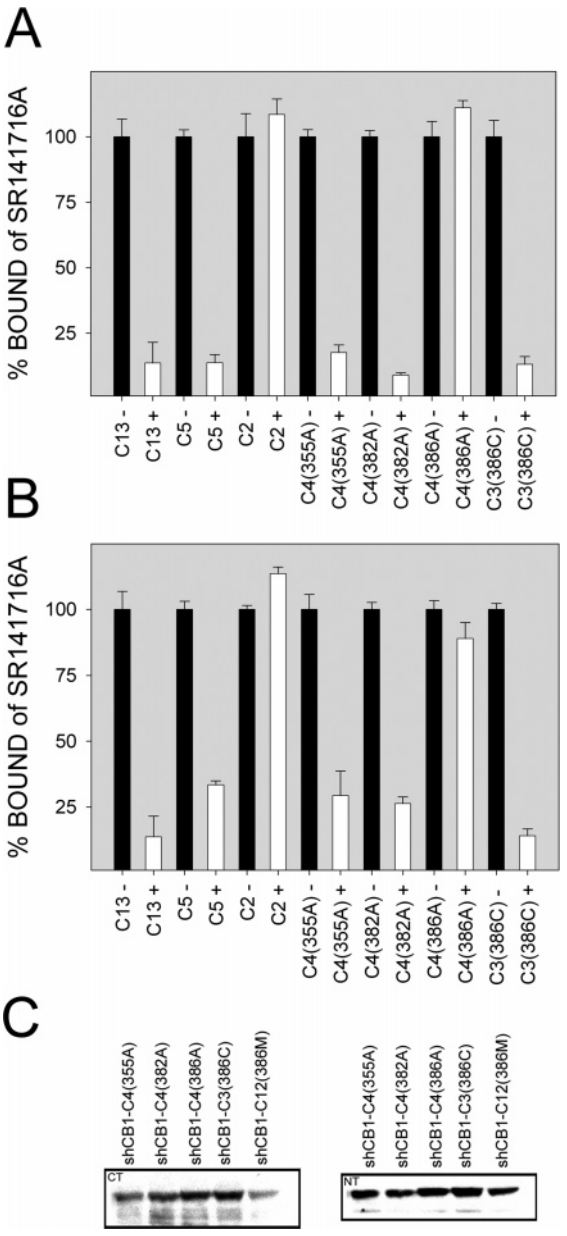

FIGURE 5: MTS reactivity at residue C386 blocks antagonist binding. The data represent the specific percent of bound [^{3}H]SR141716A for binding to 25 μg of total membrane protein from transiently expressed COS-1 cells either with (+) or without (−) a 10 min application of 50 mM MMTS (A) or 20 mM MTSEA (B). As can be seen, the presence of residue C386 makes the receptors sensitive to both MTS reagents. The means and SEM are shown for the average normalized minimum and maximum binding values. For more details, see Experimental Procedures. (C) Western blot data indicating the presence of N- and C-termini for cysteine mutants discussed above and in the legend of Figure 6.

COS-1 cells and bound agonist with wild-type-like affinities (Figure 6A). However, as anticipated, antagonist binding for shCB1-C12-C386M was severely impaired (Figure 6B). To further assess the effect of the C386M mutation on SR141716A binding, we carried out heterologous binding assays that assessed the ability of SR141716A to displace tritiated CP55940. These results indicate the C386M mutation lowers the apparent affinity for SR141716A, as judged by the K_i, approximately 5-fold compared to that of wild-type shCB1-C13 (Figure 6C). Further heterologous binding assays showed the agonist WIN55212-2 can also displace tritiated CP55940, and this behavior is unaffected by the C386M mutation (data not shown).

DISCUSSION

In this work, we examined the role of the cysteine residues in CB1, using a combination of mutagenesis and sulfhydryl reactivity studies. Our observations, and their implications for CB1 structure and function, are discussed below.

Only Residues C257 and C264 Are Required for a Functional CB1 Receptor. The human cannabinoid receptor (CB1) contains 13 cysteine residues dispersed throughout the protein (Figure 1B). As shown in Figure 1A, five of these residues appear to be highly conserved. We found that a CB1 mutant containing only the five conserved cysteine residues, shCB1-C5, and its G-protein fusion construct, shCB1-C5−$G\alpha_i$, binds agonist and antagonist and couples to the $G\alpha_i$ subunit like the wild-type shCB1-C13 receptor (see Tables 2 and 3). Together, these results indicate nonconserved cysteine residues in CB1 are not required for ligand binding and coupling to G-proteins. Similarly, mutant shCB1-C2, which contains only two cysteines thought to be involved in a disulfide bond, can also bind ligands and couple with G-proteins.

In contrast, removing all of the cysteines severely impairs the CB1 receptor, as demonstrated by mutant shCB1-C0 (see Figure 2, Table 2, Figure 3, and Table 3). Our results suggest that a disulfide bond exists between C257 and C264. To further test this possibility, we have carried out some preliminary experiments to assess the DTT sensitivity of our cysteine mutants. In our hands, we find CB1 is somewhat resistant to reduction. However, we find pretreatments with DTT (at 100 mM for 20 min) inhibit binding of agonist CP55940 to shCB1-C13 and shCB1-C2, as well as CB1 receptors present in membranes prepared from rat cortices (data not shown). Although preliminary, these results lend further support to the theory that a disulfide bond is important for agonist binding to the cannabinoid receptor. Our results clearly show that residues C257 and C264 are important for

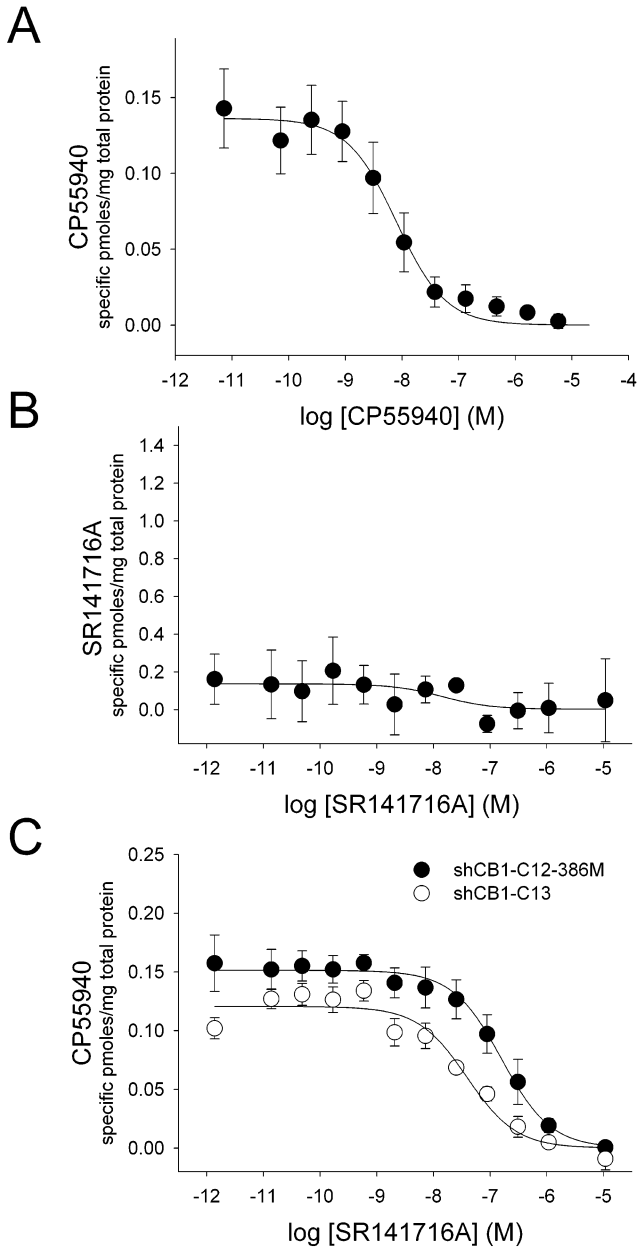

FIGURE 6: Steric bulk at C386 blocks antagonist SR141716A binding but not agonist CP55940 binding. Competitive displacement binding of mutant shCB1-C12-386M. (A) Agonist (CP55940) binding exhibits a K_d of 8 ± 4 nM. (B) In contrast, antagonist (SR141716A) binding to the same sample is severely impaired. A possible reason why the C386M mutation perturbs antagonist SR141716A binding but not agonist CP55940 binding is discussed in the text and in the legend of Figure 7. (C) Comparison of heterologous binding assays carried out on shCB1-C12-386M (●) vs shCB1-C13 (○). The data indicate the K_i for mutant shCB1-C12-386M is 194 ± 1.3 nM, compared to the value of 39 ± 0.8 nM measured for wild-type shCB1-C13. These experiments indicate that SR141716A can displace radiolabeled CP55940; however, the K_i is ~5-fold greater than that of shCB1-C13.

a functional cannabinoid receptor, and taken together, they support (but do not prove) the hypothesis that these cysteine residues are involved in a disulfide bond that stabilizes a ligand recognizable conformation of the receptor (*18*, *29*). However, direct chemical evidence proving the presence of a disulfide bond between these two residues is still needed.

Our results indicate most of the cysteine residues in CB1 are unnecessary for protein expression, ligand binding, and G-protein coupling. However, they do not rule out other structural or functional roles for the extracellular and cytoplasmic cysteine residues. For example, a cysteine in the cytoplasmic tail immediately following TMH VII is conserved in some CB1 receptors (Figure 1). It is likely that this residue is palmitoylated in CB1. What role might palmitoylation of this residue play in CB1 structure or function? Palmitoylation of analogous cysteine residues in other GPCRs has been proposed to help anchor the C-terminal tail to the membrane surface. In rhodopsin, this juxtamembrane region has been shown to form a membrane-associated helix, called "helix 8". However, the role of helix 8 palmitoylation in rhodopsin is still not clear. In one set of studies, palmitoylation does not appear to significantly affect the ability of rhodopsin to activate the G-protein (*30*), yet in another set of studies, palmitoylation induces an enhancement of activation (*31*).

Studies using peptide analogues of helix 8 for both rhodopsin and CB1 suggest this region is involved in G-protein activation (*32*−*34*). Furthermore, mutating this putative palmitoylation region in CB2 also alters signal transduction (as measured by the level of inhibition of cAMP accumulation) but does not affect ligand binding or receptor desensitization (*35*). As noted above, we observe no significant effect on ligand binding or stimulated GTPγS binding in our CB1 mutants that lack the putative palmitoylation site. However, our studies use a G-protein tethered to the CB1 receptor, which may mask any change in signaling due to mutation of the palmitoylation site. Thus, our results do not rule out a possible role for palmitoylation at C415 in the CB1 receptor.

Residue C386 (C7.42) Is Solvent Accessible and Reacts with MTS Reagents. Our cysteine reactivity studies show that MMTS and MTSEA labeling agents abolish antagonist binding in wild-type CB1 (Figure 4). Residue C386 appears to be responsible for this sensitivity, since mutating it to an alanine abolishes all effects of the MTS labels, and introducing it back into the nonreactive mutant shCB1-C2 (mutant shCB1-C3-386C) restores sensitivity to MTS agents (Figure 5).[3] Since MTS reagents primarily react only with ionized thiolates present in water-accessible regions (*26*, *36*), these results indicate residue C386 (or C7.42) must be in a water accessible microenvironment. Intriguingly, a water molecule (HOH964) is located within contact of the analogous site in the rhodopsin crystal structure (*37*).

Residue C386 Is in the Antagonist SR141716A Binding Site. Why is the binding of antagonist SR141716A so sensitive to labeling of site C386 (7.42)? The most likely explanation is that extra bulk at C386 clashes with the piperidine ring of SR141716A (personal communication with D. P. Hurst and P. H. Reggio). In agreement with this hypothesis, introducing steric bulk at this site via a C386M mutation also impedes antagonist binding, but NOT agonist binding (Figure 6). This possible clash, illustrated in Figure 7, agrees with previous work which found that substitutions at the site of the piperidine ring are deleterious to antagonist binding (*19*, *38*, *39*). Interestingly, since the C386A mutation does not alter either agonist or antagonist ligand binding,

[3] Note that other cysteine residues in CB1 may still be labeled by the MTS reagents; however, if they are, they do not alter antagonist binding.

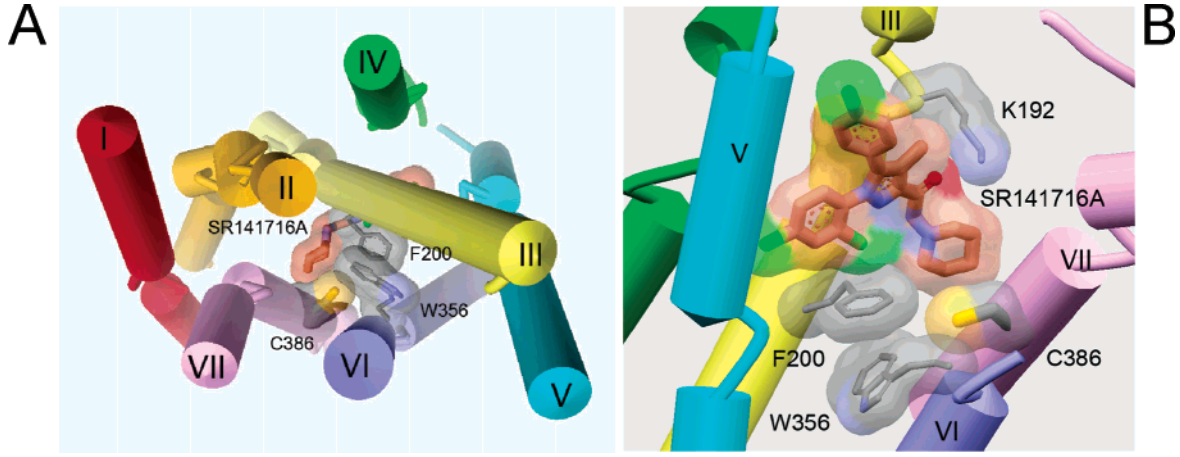

FIGURE 7: Modeling studies of SR141716A bound to CB1 suggesting there is no room for extra steric bulk at C386. Antagonist SR141716A docked in a computer model of the CB1 inactive state. (A) Model showing antagonist SR141716A bound within the transmembrane helices (TMHs) of the human cannabinoid receptor, as viewed from the intracellular surface. The helices are labeled and color-coded as in Figure 1B. The model indicates the SR141716A (orange) and key residues C386, W356, F200, and K192 with their individual solvent accessible surface. The model suggests SR141716A makes contact with these key residues in TMH III, VI, and VII. (B) Close-up view of SR141716A binding, as viewed from inside the membrane, looking from the outside of the bundle toward TMH III. Note that parts of TMH I, II, and VI have been omitted for clarity. The model clearly suggests the piperidine ring of SR141716A is in the proximity of residue C386, and thus, addition of steric bulk at this site may impair antagonist binding. In addition, as discussed in the text, introduction of steric bulk at residue 386 may also perturb nearby residues F200 (3.36) and W356 (6.48), and thus alter a critical aromatic microdomain (rotamer toggle switch) thought be involved in binding (*28*, *40*). The initial coordinates for an empty inactive CB1 receptor were kindly provided by O. Salo (*27*). Further details of the modeling procedures are given in Experimental Procedures.

residue C386 itself must not be directly required for binding of either of these ligands.

We note that our data are also consistent with an alternative SR141716A docking model recently proposed by Salo et al. (*27*). Our docking studies, using a modified version of their CB1 model (shown in Figure 7), suggest introducing steric bulk at C386 (C7.42) could also perturb important aromatic stacking interactions thought to be involved in SR141716A binding (*28*), because residue C386 is close to two key residues, F279 (F3.36) and W356 (W6.48). Previously, mutating either of these two residues to alanine has been shown to perturb antagonist (SR141716A) binding, but not agonist (CP55940) binding (*40*). In summary, our results indicate an antagonist binding determinant lies within TMH VII of the CB1 receptor, specifically at site C386 (7.42). Introducing steric bulk at this site appears to impair antagonist SR141716A binding due to clashing with the piperidine ring and/or disruption of key aromatic residues in the binding pocket. In contrast, steric bulk at this position does not affect binding of agonist CP55940.

The Region around C386 (7.42) in TMH VII May Play a Key Role in Constraining GPCR Activation. Interestingly, this region around C386 (7.42) in TMH VII appears to be crucial for antagonist binding in a number of other GPCR systems. For example, mutating the analogous residue at 7.42 from a glycine to a cysteine in the dopamine D2 receptor impairs antagonist binding (*41*), and mutagenesis studies indicate nearby residue 7.39 is an important antagonist binding determinant in the α-2-adrenergic, β-2-adrenergic, and 5-HT_{1A} receptors (*42*−*45*) as well as nearby residues 7.38 and 7.40 in 5-HT_{2A} receptors (*46*). MTS labeling studies show a cysteine at position 7.42 is sensitive to MTS labeling in the human A_1 adenosine receptor (*47*), as are nearby residues 7.35 and 7.38 in the dopamine D2 and D4 receptors (*48*), as well as a cysteine residue at position 7.38 in the μ, δ, and κ opioid receptors (*49*). Finally, we note site 7.42 is immediately adjacent to the retinal attachment site in rhodopsin (7.43), which is well established to play a key role in keeping the visual receptor in an inactive state.

Similarly, we note that a number of naturally occurring mutations within TMH VII result in constitutive activity and disease. In rhodopsin, TMH VII is normally linked to TMH III through a salt bridge between K296 (7.43) and E113 (3.28), and it is thought that this important restraint must be removed to enable receptor activation (*50*, *51*). Naturally occurring mutations in and near this salt bridge, A292E (7.39) and K296E (7.43), produce constitutively active receptors and the disease *retinitis pigmentosa* (*52*, *53*). Analogously, in the human thyrotropin receptor, the N670S mutation (7.45) is thought to be involved in hyperplasia associated with hyperthyroidism and adenoma (*54*).

Why is this region of TMH VII so sensitive to mutation and important for antagonist binding? One intriguing possibility is that it may act to keep GPCRs in an inactive state, by constraining movements of TMH VI. Such a constraint would be important because TMH VI is thought to play a key role GPCR activation, by undergoing a rigid-body movement and/or rotation of TMH VI outward relative to TMH III (*55*−*59*). It is thought that this movement results in exposure of a hydrophobic binding site(s), for the G-protein (*60*, *61*).

Thus, some change or movement of TMH VII may be required to allow the outward movement of TMH VI. Evidence for TMH VII movements in rhodopsin includes EPR and fluorescence studies (*62*−*65*), and the exposure of a region within TMH VII, the highly conserved NPXXY motif (*66*), which alters its functional ability to couple to the highly conserved DRY motif in TMH III (*67*). We propose that the interactions of antagonist in CB1, and GPCRs in general, act to inhibit GPCR activation by constraining movement of TMH VII, which in turn keeps the receptor in an inactive state, by limiting the outward movement of TMH VI. Such a constraint would limit transient exposure of the critical DRY and NPXXY motifs

in TMH III and TMH VII, as well as maintain ionic interaction between D6.30 and R3.50 (*68*, *69*), and thus inhibit receptor coupling with G-proteins. We note that our proposal is consistent with previous hypotheses about GPCR structure and mechanisms of activation (*70*−*75*).

The ability to "lock down" a GPCR, through use of antagonists or inverse agonists that block these helical movements, is an exciting prospect for the management of diseases linked to constitutively active GPCRs. However, such an approach needs an understanding of antagonist receptor interactions at the molecular level, to enable the rational approach to drug design and the selection of combinatorial chemistry libraries. Chemically reactive CB1 agonists have been described (*76*). One exciting possibility would be to functionalize the piperidine ring of SR141716A (with a thiol reactive group), thus enabling it to covalently attach to residue C386. This might further improve the activity of the antagonist SR141716A (also known as Rimonabant or Accomplia), which is showing promise as an antiobesity drug in phase III clinical trials (*77*).

Conclusions and Summary. We have shown that all but two of the 13 cysteine residues in CB1 (C257 and C264) can be replaced with alanines and still yield a functionally active receptor. We have also demonstrated that the substituted cysteine accessibility method, or SCAM (*26*, *78*, *79*), can be carried out to study the structure and function of the CB1 receptor. Our initial mutagenesis and SCAM studies clearly indicate that an endogenous cysteine residue in TMH VII, C386 (7.42), is part of a solvent-exposed binding region for the antagonist SR141716A. The sensitivity of this site to steric bulk provides experimental support for current modeling and structure−activity relationship paradigms for the cannabinoid receptor (*11*, *19*, *27*, *80*, *81*). We hope the approaches outlined here will prove useful for mapping other key determinants in CB1 function, as well as the intriguing question of CB1 attenuation (*82*, *83*).

ACKNOWLEDGMENT

We are grateful to Dr. D. P. Hurst, Dr. P. H. Reggio, Dr. Sonders, and members of the Farrens laboratory (Dr. Janz, S. E. Mansoor, and M. E. Sommer) for helpful suggestions and comments during the course of this work. Coordinates for the receptor model used in this paper are available from the corresponding author upon request.

REFERENCES

1. Reggio, P. H. (2003) Pharmacophores for ligand recognition and activation/inactivation of the cannabinoid receptors, *Curr. Pharm. Des. 9*, 1607−1633.
2. Di Marzo, V., Goparaju, S. K., Wang, L., Liu, J., Batkai, S., Jarai, Z., Fezza, F., Miura, G. I., Palmiter, R. D., Sugiura, T., and Kunos, G. (2001) Leptin-regulated endocannabinoids are involved in maintaining food intake, *Nature 410*, 822−825.
3. Kreitzer, A. C., and Regehr, W. G. (2001) Retrograde inhibition of presynaptic calcium influx by endogenous cannabinoids at excitatory synapses onto Purkinje cells, *Neuron 29*, 717−727.
4. Wilson, R. I., and Nicoll, R. A. (2001) Endogenous cannabinoids mediate retrograde signalling at hippocampal synapses, *Nature 410*, 588−592.
5. Ohno-Shosaku, T., Maejima, T., and Kano, M. (2001) Endogenous cannabinoids mediate retrograde signals from depolarized postsynaptic neurons to presynaptic terminals, *Neuron 29*, 729−738.
6. Cravatt, B. F., Giang, D. K., Mayfield, S. P., Boger, D. L., Lerner, R. A., and Gilula, N. B. (1996) Molecular characterization of an enzyme that degrades neuromodulatory fatty-acid amides, *Nature 384*, 83−87.
7. Di Marzo, V., Fontana, A., Cadas, H., Schinelli, S., Cimino, G., Schwartz, J. C., and Piomelli, D. (1994) Formation and inactivation of endogenous cannabinoid anandamide in central neurons, *Nature 372*, 686−691.
8. Stella, N., Schweitzer, P., and Piomelli, D. (1997) A second endogenous cannabinoid that modulates long-term potentiation, *Nature 388*, 773−778.
9. Andersson, H., D'Antona, A. M., Kendall, D. A., Von Heijne, G., and Chin, C. N. (2003) Membrane assembly of the cannabinoid receptor 1: Impact of a long N-terminal tail, *Mol. Pharmacol. 64*, 570−577.
10. Murphy, J. W., and Kendall, D. A. (2003) Integrity of extracellular loop 1 of the human cannabinoid receptor 1 is critical for high-affinity binding of the ligand CP 55,940 but not SR 141716A, *Biochem. Pharmacol. 65*, 1623−1631.
11. Hurst, D. P., Lynch, D. L., Barnett-Norris, J., Hyatt, S. M., Seltzman, H. H., Zhong, M., Song, Z. H., Nie, J., Lewis, D., and Reggio, P. H. (2002) N-(Piperidin-1-yl)-5-(4-chlorophenyl)-1-(2,4-dichlorophenyl)-4-methyl-1H-pyrazole-3-carboxamide (SR141716A) interaction with LYS 3.28(192) is crucial for its inverse agonism at the cannabinoid CB1 receptor, *Mol. Pharmacol. 62*, 1274−1287.
12. Palczewski, K., Kumasaka, T., Hori, T., Behnke, C. A., Motoshima, H., Fox, B. A., Le Trong, I., Teller, D. C., Okada, T., Stenkamp, R. E., Yamamoto, M., and Miyano, M. (2000) Crystal structure of rhodopsin: A G protein-coupled receptor, *Science 289*, 739−745.
13. Karnik, S. S., and Khorana, H. G. (1990) Assembly of functional rhodopsin requires a disulfide bond between cysteine residues 110 and 187, *J. Biol. Chem. 265*, 17520−17524.
14. Ridge, K. D., Lu, Z., Liu, X., and Khorana, H. G. (1995) Structure and function in rhodopsin. Separation and characterization of the correctly folded and misfolded opsins produced on expression of an opsin mutant gene containing only the native intradiscal cysteine codons, *Biochemistry 34*, 3261−3267.
15. Hwa, J., Reeves, P. J., Klein-Seetharaman, J., Davidson, F., and Khorana, H. G. (1999) Structure and function in rhodopsin: Further elucidation of the role of the intradiscal cysteines, Cys-110, -185, and -187, in rhodopsin folding and function, *Proc. Natl. Acad. Sci. U.S.A. 96*, 1932−1935.
16. Hwa, J., Klein-Seetharaman, J., and Khorana, H. G. (2001) Structure and function in rhodopsin: Mass spectrometric identification of the abnormal intradiscal disulfide bond in misfolded retinitis pigmentosa mutants, *Proc. Natl. Acad. Sci. U.S.A. 98*, 4872−4876.
17. Lu, R., Hubbard, J. R., Martin, B. R., and Kalimi, M. Y. (1993) Roles of sulfhydryl and disulfide groups in the binding of CP-55,940 to rat brain cannabinoid receptor, *Mol. Cell. Biochem. 121*, 119−126.
18. Shire, D., Calandra, B., Delpech, M., Dumont, X., Kaghad, M., Le Fur, G., Caput, D., and Ferrara, P. (1996) Structural features of the central cannabinoid CB1 receptor involved in the binding of the specific CB1 antagonist SR 141716A, *J. Biol. Chem. 271*, 6941−6946.
19. Francisco, M. E., Seltzman, H. H., Gilliam, A. F., Mitchell, R. A., Rider, S. L., Pertwee, R. G., Stevenson, L. A., and Thomas, B. F. (2002) Synthesis and structure−activity relationships of amide and hydrazide analogues of the cannabinoid CB(1) receptor antagonist N-(piperidinyl)-5-(4-chlorophenyl)-1-(2,4-dichlorophenyl)-4-methyl-1H-pyrazole-3-carboxamide (SR141716), *J. Med. Chem. 45*, 2708−2719.
20. Ballesteros, J. A., and Weinstein, H. (1995) Integrated Methods for Modeling G-Protein Coupled Receptors, *Methods Neurosci. 25*, 366−428.
21. Farrens, D. L., Dunham, T. D., Fay, J. F., Dews, I. C., Caldwell, J., and Nauert, B. (2002) Design, expression, and characterization of a synthetic human cannabinoid receptor and cannabinoid receptor/G-protein fusion protein, *J. Pept. Res. 60*, 336−347.
22. Oprian, D. D., Molday, R. S., Kaufman, R. J., and Khorana, H. G. (1987) Expression of a synthetic bovine rhodopsin gene in monkey kidney cells, *Proc. Natl. Acad. Sci. U.S.A. 84*, 8874−8878.
23. Janz, J. M., Fay, J. F., and Farrens, D. L. (2003) Stability of dark state rhodopsin is mediated by a conserved ion pair in intradiscal loop E-2, *J. Biol. Chem. 278*, 16982−16991.
24. Swillens, S. (1995) Interpretation of binding curves obtained with high receptor concentrations: Practical aid for computer analysis, *Mol. Pharmacol. 47*, 1197−1203.

25. DeBlasi, A., O'Reilly, K., and Motulsky, H. J. (1989) Calculating receptor number from binding experiments using same compound as radioligand and competitor, *Trends Pharmacol. Sci. 10*, 227−229.
26. Javitch, J. A., Shi, L., and Liapakis, G. (2002) Use of the substituted cysteine accessibility method to study the structure and function of G protein-coupled receptors, *Methods Enzymol. 343*, 137−156.
27. Salo, O. M., Lahtela-Kakkonen, M., Gynther, J., Jarvinen, T., and Poso, A. (2004) Development of a 3D model for the human cannabinoid CB1 receptor, *J. Med. Chem. 47*, 3048−3057.
28. Singh, R., Hurst, D. P., Barnett-Norris, J., Lynch, D. L., Reggio, P. H., and Guarnieri, F. (2002) Activation of the cannabinoid CB1 receptor may involve a W6 48/F3 36 rotamer toggle switch, *J. Pept. Res. 60*, 357−370.
29. Gouldson, P., Calandra, B., Legoux, P., Kerneis, A., Rinaldi-Carmona, M., Barth, F., Le Fur, G., Ferrara, P., and Shire, D. (2000) Mutational analysis and molecular modelling of the antagonist SR 144528 binding site on the human cannabinoid CB(2) receptor, *Eur. J. Pharmacol. 401*, 17−25.
30. Karnik, S. S., Ridge, K. D., Bhattacharya, S., and Khorana, H. G. (1993) Palmitoylation of bovine opsin and its cysteine mutants in COS cells, *Proc. Natl. Acad. Sci. U.S.A. 90*, 40−44.
31. Morrison, D. F., O'Brien, P. J., and Pepperberg, D. R. (1991) Depalmitylation with hydroxylamine alters the functional properties of rhodopsin, *J. Biol. Chem. 266*, 20118−20123.
32. Marin, E. P., Krishna, A. G., Zvyaga, T. A., Isele, J., Siebert, F., and Sakmar, T. P. (2000) The amino terminus of the fourth cytoplasmic loop of rhodopsin modulates rhodopsin-transducin interaction, *J. Biol. Chem. 275*, 1930−1936.
33. Howlett, A. C., Song, C., Berglund, B. A., Wilken, G. H., and Pigg, J. J. (1998) Characterization of CB1 cannabinoid receptors using receptor peptide fragments and site-directed antibodies, *Mol. Pharmacol. 53*, 504−510.
34. Mukhopadhyay, S., Cowsik, S. M., Lynn, A. M., Welsh, W. J., and Howlett, A. C. (1999) Regulation of Gi by the CB1 cannabinoid receptor C-terminal juxtamembrane region: Structural requirements determined by peptide analysis, *Biochemistry 38*, 3447−3455.
35. Feng, W., and Song, Z. H. (2001) Functional roles of the tyrosine within the NP(X)(n)Y motif and the cysteines in the C-terminal juxtamembrane region of the CB2 cannabinoid receptor, *FEBS Lett. 501*, 166−170.
36. Roberts, D. D., Lewis, S. D., Ballou, D. P., Olson, S. T., and Shafer, J. A. (1986) Reactivity of small thiolate anions and cysteine-25 in papain toward methyl methanethiosulfonate, *Biochemistry 25*, 5595−5601.
37. Okada, T., Fujiyoshi, Y., Silow, M., Navarro, J., Landau, E. M., and Shichida, Y. (2002) Functional role of internal water molecules in rhodopsin revealed by X-ray crystallography, *Proc. Natl. Acad. Sci. U.S.A. 99*, 5982−5987.
38. Wiley, J. L., Jefferson, R. G., Grier, M. C., Mahadevan, A., Razdan, R. K., and Martin, B. R. (2001) Novel pyrazole cannabinoids: Insights into CB(1) receptor recognition and activation, *J. Pharmacol. Exp. Ther. 296*, 1013−1022.
39. Lan, R., Liu, Q., Fan, P., Lin, S., Fernando, S. R., McCallion, D., Pertwee, R., and Makriyannis, A. (1999) Structure−activity relationships of pyrazole derivatives as cannabinoid receptor antagonists, *J. Med. Chem. 42*, 769−776.
40. McAllister, S. D., Rizvi, G., Anavi-Goffer, S., Hurst, D. P., Barnett-Norris, J., Lynch, D. L., Reggio, P. H., and Abood, M. E. (2003) An aromatic microdomain at the cannabinoid CB(1) receptor constitutes an agonist/inverse agonist binding region, *J. Med. Chem. 46*, 5139−5152.
41. Fu, D., Ballesteros, J. A., Weinstein, H., Chen, J., and Javitch, J. A. (1996) Residues in the seventh membrane-spanning segment of the dopamine D2 receptor accessible in the binding-site crevice, *Biochemistry 35*, 11278−11285.
42. Guan, X. M., Peroutka, S. J., and Kobilka, B. K. (1992) Identification of a single amino acid residue responsible for the binding of a class of β-adrenergic receptor antagonists to 5-hydroxytryptamine 1A receptors, *Mol. Pharmacol. 41*, 695−698.
43. Suryanarayana, S., Daunt, D. A., Von Zastrow, M., and Kobilka, B. K. (1991) A single point mutation in the seventh hydrophobic domain of the α2-adrenergic receptor changes antagonist binding specificity to that of a β receptor, *Trans. Assoc. Am. Physicians 104*, 62−68.
44. Suryanarayana, S., Daunt, D. A., Von Zastrow, M., and Kobilka, B. K. (1991) A point mutation in the seventh hydrophobic domain of the α2 adrenergic receptor increases its affinity for a family of β receptor antagonists, *J. Biol. Chem. 266*, 15488−15492.
45. Suryanarayana, S., and Kobilka, B. K. (1993) Amino acid substitutions at position 312 in the seventh hydrophobic segment of the β2-adrenergic receptor modify ligand-binding specificity, *Mol. Pharmacol. 44*, 111−114.
46. Roth, B. L., Shoham, M., Choudhary, M. S., and Khan, N. (1997) Identification of conserved aromatic residues essential for agonist binding and second messenger production at 5-hydroxytryptamine 2A receptors, *Mol. Pharmacol. 52*, 259−266.
47. Dawson, E. S., and Wells, J. N. (2001) Determination of amino acid residues that are accessible from the ligand binding crevice in the seventh transmembrane-spanning region of the human A(1) adenosine receptor, *Mol. Pharmacol. 59*, 1187−1195.
48. Simpson, M. M., Ballesteros, J. A., Chiappa, V., Chen, J., Suehiro, M., Hartman, D. S., Godel, T., Snyder, L. A., Sakmar, T. P., and Javitch, J. A. (1999) Dopamine D4/D2 receptor selectivity is determined by a divergent aromatic microdomain contained within the second, third, and seventh membrane-spanning segments, *Mol. Pharmacol. 56*, 1116−1126.
49. Xu, W., Chen, C., Huang, P., Li, J., de Riel, J. K., Javitch, J. A., and Liu-Chen, L. Y. (2000) The conserved cysteine 7.38 residue is differentially accessible in the binding-site crevices of the μ, δ, and κ opioid receptors, *Biochemistry 39*, 13904−13915.
50. Rao, V. R., and Oprian, D. D. (1996) Activating mutations of rhodopsin and other G protein-coupled receptors, *Annu. Rev. Biophys. Biomol. Struct. 25*, 287−314.
51. Kim, J. M., Altenbach, C., Kono, M., Oprian, D. D., Hubbell, W. L., and Khorana, H. G. (2004) Structural origins of constitutive activation in rhodopsin: Role of the K296/E113 salt bridge, *Proc. Natl. Acad. Sci. U.S.A. 101*, 12508−12513.
52. Dryja, T. P., Berson, E. L., Rao, V. R., and Oprian, D. D. (1993) Heterozygous missense mutation in the rhodopsin gene as a cause of congenital stationary night blindness, *Nat. Genet. 4*, 280−283.
53. Robinson, P. R., Cohen, G. B., Zhukovsky, E. A., and Oprian, D. D. (1992) Constitutively active mutants of rhodopsin, *Neuron 9*, 719−725.
54. Tonacchera, M., Van Sande, J., Cetani, F., Swillens, S., Schvartz, C., Winiszewski, P., Portmann, L., Dumont, J. E., Vassart, G., and Parma, J. (1996) Functional characteristics of three new germline mutations of the thyrotropin receptor gene causing autosomal dominant toxic thyroid hyperplasia, *J. Clin. Endocrinol. Metab. 81*, 547−554.
55. Altenbach, C., Yang, K., Farrens, D. L., Farahbakhsh, Z. T., Khorana, H. G., and Hubbell, W. L. (1996) Structural features and light-dependent changes in the cytoplasmic interhelical E−F loop region of rhodopsin: A site-directed spin-labeling study, *Biochemistry 35*, 12470−12478.
56. Farrens, D. L., Altenbach, C., Yang, K., Hubbell, W. L., and Khorana, H. G. (1996) Requirement of rigid-body motion of transmembrane helices for light activation of rhodopsin, *Science 274*, 768−770.
57. Sheikh, S. P., Zvyaga, T. A., Lichtarge, O., Sakmar, T. P., and Bourne, H. R. (1996) Rhodopsin activation blocked by metal-ion-binding sites linking transmembrane helices C and F, *Nature 383*, 347−350.
58. Gether, U., Lin, S., Ghanouni, P., Ballesteros, J. A., Weinstein, H., and Kobilka, B. K. (1997) Agonists induce conformational changes in transmembrane domains III and VI of the β2 adrenoceptor, *EMBO J. 16*, 6737−6747.
59. Dunham, T. D., and Farrens, D. L. (1999) Conformational changes in rhodopsin. Movement of helix f detected by site-specific chemical labeling and fluorescence spectroscopy, *J. Biol. Chem. 274*, 1683−1690.
60. Janz, J. M., and Farrens, D. L. (2004) Rhodopsin activation exposes a key hydrophobic binding site for the transducin α-subunit C terminus, *J. Biol. Chem. 279*, 29767−29773.
61. Ulfers, A. L., McMurry, J. L., Miller, A., Wang, L., Kendall, D. A., and Mierke, D. F. (2002) Cannabinoid receptor-G protein interactions: $G_{\alpha i1}$-bound structures of IC3 and a mutant with altered G protein specificity, *Protein Sci. 11*, 2526−2531.
62. Yang, K., Farrens, D. L., Altenbach, C., Farahbakhsh, Z. T., Hubbell, W. L., and Khorana, H. G. (1996) Structure and function in rhodopsin. Cysteines 65 and 316 are in proximity in a rhodopsin mutant as indicated by disulfide formation and interactions between attached spin labels, *Biochemistry 35*, 14040−14046.

63. Hubbell, W. L., Altenbach, C., Hubbell, C. M., and Khorana, H. G. (2003) Rhodopsin structure, dynamics, and activation: A perspective from crystallography, site-directed spin labeling, sulfhydryl reactivity, and disulfide cross-linking, *Adv. Protein Chem. 63*, 243−290.
64. Alexiev, U., Rimke, I., and Pohlmann, T. (2003) Elucidation of the nature of the conformational changes of the EF-interhelical loop in bacteriorhodopsin and of the helix VIII on the cytoplasmic surface of bovine rhodopsin: A time-resolved fluorescence depolarization study, *J. Mol. Biol. 328*, 705−719.
65. Imamoto, Y., Kataoka, M., Tokunaga, F., and Palczewski, K. (2000) Light-induced conformational changes of rhodopsin probed by fluorescent alexa594 immobilized on the cytoplasmic surface, *Biochemistry 39*, 15225−15233.
66. Abdulaev, N. G., and Ridge, K. D. (1998) Light-induced exposure of the cytoplasmic end of transmembrane helix seven in rhodopsin, *Proc. Natl. Acad. Sci. U.S.A. 95*, 12854−12859.
67. Fritze, O., Filipek, S., Kuksa, V., Palczewski, K., Hofmann, K. P., and Ernst, O. P. (2003) Role of the conserved NPxxY(x)5,6F motif in the rhodopsin ground state and during activation, *Proc. Natl. Acad. Sci. U.S.A. 100*, 2290−2295.
68. Shapiro, D. A., Kristiansen, K., Weiner, D. M., Kroeze, W. K., and Roth, B. L. (2002) Evidence for a model of agonist-induced activation of 5-hydroxytryptamine 2A serotonin receptors that involves the disruption of a strong ionic interaction between helices 3 and 6, *J. Biol. Chem. 277*, 11441−11449.
69. Ballesteros, J. A., Jensen, A. D., Liapakis, G., Rasmussen, S. G., Shi, L., Gether, U., and Javitch, J. A. (2001) Activation of the β2-adrenergic receptor involves disruption of an ionic lock between the cytoplasmic ends of transmembrane segments 3 and 6, *J. Biol. Chem. 276*, 29171−29177.
70. Gerber, B. O., Meng, E. C., Dotsch, V., Baranski, T. J., and Bourne, H. R. (2001) An activation switch in the ligand binding pocket of the C5a receptor, *J. Biol. Chem. 276*, 3394−3400.
71. Teller, D. C., Stenkamp, R. E., and Palczewski, K. (2003) Evolutionary analysis of rhodopsin and cone pigments: Connecting the three-dimensional structure with spectral tuning and signal transfer, *FEBS Lett. 555*, 151−159.
72. Karnik, S. S., Gogonea, C., Patil, S., Saad, Y., and Takezako, T. (2003) Activation of G-protein-coupled receptors: A common molecular mechanism, *Trends Endocrinol. Metab. 14*, 431−437.
73. Ballesteros, J. A., Shi, L., and Javitch, J. A. (2001) Structural mimicry in G protein-coupled receptors: Implications of the high-resolution structure of rhodopsin for structure−function analysis of rhodopsin-like receptors, *Mol. Pharmacol. 60*, 1−19.
74. Visiers, I., Ballesteros, J. A., and Weinstein, H. (2002) Three-dimensional representations of G protein-coupled receptor structures and mechanisms, *Methods Enzymol. 343*, 329−371.
75. Swaminath, G., Xiang, Y., Lee, T. W., Steenhuis, J., Parnot, C., and Kobilka, B. K. (2004) Sequential binding of agonists to the β2 adrenoceptor. Kinetic evidence for intermediate conformational states, *J. Biol. Chem. 279*, 686−691.
76. Picone, R. P., Fournier, D. J., Makriyannis, A. (2002) Ligand based structural studies of the CB1 cannabinoid receptor. *J. Pept. Res. 60*, 348−356.
77. Bays, H. E. (2004) Current and investigational antiobesity agents and obesity therapeutic treatment targets, *Obes. Res. 12*, 1197−1211.
78. Karlin, A., and Akabas, M. H. (1998) Substituted-cysteine accessibility method, *Methods Enzymol. 293*, 123−145.
79. Akabas, M. H., Stauffer, D. A., Xu, M., and Karlin, A. (1992) Acetylcholine receptor channel structure probed in cysteine-substitution mutants, *Science 258*, 307−310.
80. Shim, J. Y., Welsh, W. J., Cartier, E., Edwards, J. L., and Howlett, A. C. (2002) Molecular interaction of the antagonist N-(piperidin-1-yl)-5-(4-chlorophenyl)-1-(2,4-dichlorophenyl)-4-methyl-1H-pyrazole-3-carboxamide with the CB1 cannabinoid receptor, *J. Med. Chem. 45*, 1447−1459.
81. McAllister, S. D., Hurst, D. P., Barnett-Norris, J., Lynch, D., Reggio, P. H., and Abood, M. E. (2004) Structural mimicry in class A protein-coupled receptor rotamer toggle switches: The importance of the F3.36(201)/W6.48(357) interaction in cannabinoid CB1 receptor activation, *J. Biol. Chem. 279*, 48024−48037.
82. Hsieh, C., Brown, S., Derleth, C., Mackie, K. (1999) Internalization and recycling of the CB1 cannabinoid receptor. *J. Neurochem. 73*, 493−501.
83. Luk, T., Jin, W., Zvonok, A., Lu, D., Lin, X. Z., Chavkin, C., Makriyannis, A., Mackie, K. (2004) Identification of a potent and highly efficacious, yet slowly desensitizing CB1 cannabinoid receptor agonist. *Br. J. Pharmacol. 142*, 495−500.

BI0472651